THE JOURNAL OF BIOLOGICAL CHEMISTRY VOL. 285, NO. 43, pp. 32937–32945, October 22, 2010

Diversity of Innate Immune Recognition Mechanism for Bacterial Polymeric *meso*-Diaminopimelic Acid-type Peptidoglycan in Insects[S]

Received for publication, May 11, 2010, and in revised form, July 12, 2010 Published, JBC Papers in Press, August 11, 2010, DOI 10.1074/jbc.M110.144014

Yang Yu[‡1,2], Ji-Won Park[‡1], Hyun-Mi Kwon[‡], Hyun-Ok Hwang[‡], In-Hwan Jang[§], Akiko Masuda[¶‖], Kenji Kurokawa[‡], Hiroshi Nakayama[¶‖], Won-Jae Lee[§], Naoshi Dohmae[¶‖], Jinghai Zhang[**], and Bok Luel Lee[‡3]

From the [‡]National Research Laboratory of Defense Proteins, College of Pharmacy, Pusan National University, Busan 609-735, Korea, the [§]Division of Molecular Life Science, Ewha Woman's University, Seoul 120-750, Korea, the [¶]Biomolecular Characterization Team, RIKEN, Wako 351-0198, Japan, [‖]Core Research for Evolutional Science and Technology, Japan Science and Technology Agency, Tokyo 102-0075, Japan, and the [**]School of Life Science and Biopharmaceutics, Shenyang Pharmaceutical University, Shenyang 110016, China

In *Drosophila*, the synthesis of antimicrobial peptides in response to microbial infections is under the control of the Toll and immune deficiency (Imd) signaling pathway. The Toll signaling pathway responds mainly to the lysine-type peptidoglycan of Gram-positive bacteria and fungal β-1,3-glucan, whereas the Imd pathway responds to the *meso*-diaminopimelic acid (DAP)-type peptidoglycan of Gram-negative bacteria and certain Gram-positive bacilli. Recently we determined the activation mechanism of a Toll signaling pathway biochemically using a large beetle, *Tenebrio molitor*. However, DAP-type peptidoglycan recognition mechanism and its signaling pathway are still unclear in the fly and beetle. Here, we show that polymeric DAP-type peptidoglycan, but not its monomeric form, formed a complex with *Tenebrio* peptidoglycan recognition protein-SA, and this complex activated the three-step proteolytic cascade to produce processed Spätzle, a Toll receptor ligand, and induced *Drosophila* defensin-like antimicrobial peptide in *Tenebrio* larvae similarly to polymeric lysine-type peptidoglycan. Monomeric DAP-type peptidoglycan induced *Drosophila* diptericin-like antimicrobial peptide in *Tenebrio* hemocytes. In addition, both polymeric and monomeric DAP-type peptidoglycans induced expression of *Tenebrio* peptidoglycan recognition protein-SC2, which is DAP-type peptidoglycan-selective *N*-acetylmuramyl-L-alanine amidase that functions as a DAP-type peptidoglycan scavenger, appearing to function as a negative regulator of the DAP-type peptidoglycan signaling by cleaving DAP-type peptidoglycan in *Tenebrio* larvae. Taken together, these results demonstrate that molecular recognition mechanism for polymeric DAP-type peptidoglycan is different between *Tenebrio* larvae and *Drosophila* adults, providing biochemical evidences of biological diversity of innate immune responses in insects.

Peptidoglycan (PG)[4] is a microbial cell wall-associated component found only in bacteria, not in eukaryotes. Polymeric PG is composed of disaccharide GlcNAc-*N*-acetylmuramic acid linked to a stem peptide containing D- and L-amino acid residues. The third residue of the stem peptide is most lysine in Gram-positive bacteria and *meso*-diaminopimelic acid (DAP) in Gram-negative bacteria and certain Gram-positive bacilli species (1). The hallmark of *Drosophila* humoral innate immune response is the induction of antimicrobial peptide (AMP) genes in the fat body (equivalent of the mammalian liver) by microbial challenge or by injection of Lys- or DAP-type PGs (2). Recent elegant *Drosophila* genetic studies showed that the synthesis of AMPs in response to microbial infections is under the control of the Toll and immune deficiency (Imd) signaling pathway (2). The *Imd* gene encodes a 25-kDa protein with a death domain that has strong similarities to that of mammalian RIP (TNF receptor-interacting protein) (3). The biological significance of these two *Drosophila* signaling pathways is demonstrated by the fact that mutations of the genes involved in these pathways dramatically decrease resistance to microbial infections, *e.g. Toll* mutants are susceptible to fungal infections, and *Relish*, the NF-κB protein involved in Imd pathway, mutants lose resistance to Gram-negative bacterial infections (4, 5).

PG recognition protein (PGRP) family proteins are critical receptors in *Drosophila* immune responses that are required for the recognition of PG and for subsequent activation of AMP gene expression (2). PGRPs were first characterized in the moths *Bombyx mori* and *Trichoplusia ni* (6, 7) and proposed to be receptors that can trigger innate immune responses. The discovery of insect PGRPs and their immune functions prompted the search for mammalian homologues, and it is now established that mice and humans express four genes encoding members of this family (8). One of these is a small form, PGRP-S, present in granules of neutrophil. Mice in which the PGRP-S gene has been knocked out showed impaired intracellular killing of low pathogenicity Gram-positive bacte-

[S] The on-line version of this article (available at http://www.jbc.org) contains supplemental Table S1 and Figs. S1–S4.

The nucleotide sequence(s) reported in this paper has been submitted to the DDBJ/GenBank™/EBI Data Bank with accession number(s) AB560751.

[1] Both authors contributed equally to this work.

[2] Present address: School of Life Science and Biopharmaceutics, Shenyang Pharmaceutical University, Shenyang 110016, China.

[3] To whom correspondence should be addressed: National Research Laboratory of Defense Proteins, College of Pharmacy, Pusan National University, Jangjeon Dong, Gumjeong Gu, Busan 609-735, Korea. Tel.: 82-51-510-2809; Fax: 82-51-513-2801; E-mail: brlee@pusan.ac.kr.

[4] The abbreviations used are: PG, peptidoglycan; DAP, *meso*-diaminopimelic acid; AMP, antimicrobial peptides; Imd, immune deficiency; PGRP, PG recognition protein; GNBP, Gram-negative-binding protein; SP, serine protease; SPE, Spätzle processing enzyme; MSP, modular serine protease; SAE, SPE-activating enzyme; DDW, double distilled water; PO, phenoloxidase.

ria (9). PGRPs share homology with *N*-acetylmuramoyl-L-alanine amidases, which cleave PG at the lactylamide bond between the glycan backbone and the stem peptides (6). Some noncatalytic PGRPs, such as PGRP-LC, -LE, -SA, and -SD, lack a critical cysteine residue in the catalytic pocket and are not able to cleave PG (10), but these PGRPs can bind PGs and are necessary for expression of AMP genes, indicating that these PGRPs directly recognize bacteria and activate innate immune responses. In contrast, catalytic PGRPs, such as PGRP-SC1a, -LB, and -SC2, include this cysteine residue in the active site and are potent enzymes that cleave PG (10). After digestion with PGRP-SC1b, S*taphylococcal* PG exhibits less activation of the AMP genes in a *Drosophila* blood cell line, so it was hypothesized that catalytic PGRPs may act as scavengers to limit an inflammatory response to free PG (10).

The *Drosophila* Toll signaling pathway is activated upon recognition of Lys-type PG and β-1,3-glucan, which are found as major components in Gram-positive bacteria and fungi, respectively (11, 12). The Toll receptor is an evolutionarily conserved molecule that plays a key role in the establishment of the dorso-ventral axis of the *Drosophila* embryo, as well as in several other developmental processes (13). The *Drosophila* Toll pathway shares significant similarities with the intracellular signaling cascade activated downstream of mammalian interleukin-1 and Toll-like receptors, indicating a common ancestry for these immune mechanisms. Lys-type PG and β-1,3-glucan are specifically recognized by the PG recognition protein (PGRP)-SA·Gram-negative-binding protein 1 (GNBP1) complex and GNBP3, respectively. GNBPs are 50-kDa proteins with a C-terminal, 200-residue β-glucanase-like domain and an N-terminal, 100-residue domain reported to bind β-1,3-glucan (14). In contrast, the Imd pathway is activated primarily via PGRP-LC or PGRP-LE after recognition of DAP-type PG found in Gram-negative bacteria and *Bacillus* sp. (15, 16). Both pathways lead to the expression of AMPs via NF-κB-like transcription factors (2, 17, 18). The Imd pathway predominately regulates the synthesis of diptericin, which is mediated by cell surface PGRP-LC receptors and intracellular Imd adaptor protein. The Toll pathway predominantly regulates induction of the drosomycin. The minimum structure of the DAP-type PG required for activation of the PGRP-LC-mediated Imd pathway is monomeric DAP-type PG with an internal 1,6-anhydro bond, known as tracheal cytotoxin (19).

Several downstream molecules involved in the regulation of the Toll signaling pathway were identified in *Drosophila*. The processed extracellular Spätzle, a cysteine knot molecule with structural similarities to mammalian nerve growth factor (NGF), is generated from pro-Spätzle by a serine protease (SP), Spätzle processing enzyme (SPE), and functions as a ligand of the Toll receptor (20). The activation of SPE zymogen is known to be induced by sequential activation of several upstream SPs (12, 21–23). In addition, several intracellular molecules involved in the regulation of the Imd pathway are also identified by intensive *Drosophila* genetic studies (24). Although the intracellular recognition modes of the Imd pathway are relatively elucidated, the extracellular recognition mechanism of the Imd pathway is still unclear, such as how monomeric DAP-type PG is delivered to PGRP-LC or PGRP-LE and how the PGRP-LE-mediated DAP-type PG recognition signal is transferred to the Imd protein. Although the complex crystallographic structures of tracheal cytotoxin·PGRP-LC and tracheal cytotoxin·PGRP-LE complexes were dissolved, and monomeric DAP-type PG recognition modes were postulated (25, 26), the molecular recognition mechanism of polymeric DAP-type PG *in vivo* still needs to be determined.

In our recent biochemical studies using a large beetle, *Tenebrio molitor*, we demonstrated that Lys-type PG is recognized by a *Tenebrio* PGRP-SA·GNBP1 complex, whereas β-1.3-glucan is recognized by GNBP3 (27–29). Both *Tenebrio* PGRP-SA·GNBP1 complex and *Tenebrio* GNBP3 mediated the activation of a three-step proteolytic SP cascade that ultimately leads to the cleavage of pro-Spätzle into processed Spätzle (30, 31). Our work supports a model in which bacterial Lys-type PG and fungal β-1,3-glucan recognition signals activate a common proteolytic cascade involving three different SP zymogens that are sequentially processed. During these studies, the fact that we unexpectedly observed that *Tenebrio* PGRP-SA recognizes both polymeric Lys-type PGs and polymeric DAP-type PGs in an *in vitro* binding assay (28) implies that *Tenebrio* larvae may have a unique DAP-type PG recognition mechanism compared with *Drosophila* adults. Because we set out to test purification methods for homogeneous polymeric DAP-type PGs, we decided to investigate how *Tenebrio* larvae recognize DAP-type PGs, how they transfer DAP-type PG recognition signal to the downstream molecules for their host defense, and what types of AMP(s) are induced by injection of polymeric and monomeric DAP-type PGs.

To answer these questions, we examined how polymeric DAP-type and monomeric DAP-type PGs were sensed in *Tenebrio* larvae and *Drosophila* adults and what types of AMPs were induced by injection of two different DAP-type PGs into these insects. Here, we show that, unlike *Drosophila* adults, polymeric DAP-type-PGs were also recognized by the *Tenebrio* PGRP-SA·GNBP 1 complex and that the DAP-type PG·PGRP-SA·GNBP1 complex induced sequential activation of the three-step SP cascade like Lys-type PG-mediated Toll signaling pathway. However, monomeric DAP-type PGs failed to activate the *Tenebrio* Toll pathway. Furthermore, when polymeric DAP-type and Lys-type PGs were injected to *Tenebrio* larvae, these PGs induced the expression of *Tenebrio* PGRP-SA and PGRP-SC2 simultaneously in the hemolymph (insect blood), implying that *Tenebrio* larvae elegantly utilize PG sensing molecule and PG scavenger molecule simultaneously for host defense against bacterial infection. These differential innate immune responses in *Drosophila* and *Tenebrio* systems are further biochemical evidence of the biological diversity of insect innate immunity.

EXPERIMENTAL PROCEDURES

Bacterial Strains and Culture—The following bacteria strains were used: *Staphylococcus aureus* RN 4220, *Escherichia coli* K12, *Micrococcus luteus* ATCC 4698, and *Bacillus subtilis* subsp.168 strain. All of these bacterial strains were cultured with Luria-Bertani medium supplemented with antibiotics wherever required.

Injection of PGs and Collection of Hemolymphs—T. molitor larvae (mealworms) were maintained on a laboratory bench

in terraria containing wheat bran. Prior to injection of PGs, the larvae were chilled on ice for 5 min. Then 4 μl of soluble PGs was injected directly into each individual larva on the third and fourth ventral abdominal sternites. Each PG sample was injected into 20 larvae. Hemolymphs were collected as described previously (27). Briefly, to harvest the hemolymph, a larva was pricked using a 25-gauge needle, and then a 10-μl drop of hemolymph was collected in 100 μl of a modified anticoagulation buffer (136 mM trisodium citrate, 26 mM citric acid, 20 mM EDTA, and 15 mM sodium chloride, pH 5.0). The collected crude hemolymph was centrifuged at 200,000 × *g* for 15 min at 4 °C. The supernatant was then stored at −80 °C until use.

Purification of Insoluble Lys-type PGs and Polymeric DAP-type PGs—Insoluble Lys-type PGs were prepared from *S. aureus* and *M. luteus* strains according to our published method (29) with some modifications. Briefly, cultured cells were destructed with glass beads and then centrifuged to harvest supernatant at 800 × *g* for 10 min at 4 °C. The pellet was obtained from harvested supernatant by centrifugation at 13,000 × *g* for 10 min at 4 °C. Then the pellet was gently resuspended with 0.5% SDS, incubated in 60 °C for 30 min, and centrifuged at 13,000 × *g* for 10 min at room temperature. The collected pellet was washed with double distilled water (DDW) to remove SDS, and then the pellet was resuspended with 1 M Tris-HCl (pH 7.0) containing 10 mM $CaCl_2$ for trypsin treatment (final concentration, 200 μg/ml) for 12 h at 37 °C. After incubation, the pellet was collected by centrifugation at 13,000 × *g* for 10 min and then washed with 1 M Tris-HCl (pH 7.0) containing 1 M NaCl before washing with DDW three times. The residue was treated with hydrofluoric acid (final concentration, 40%) for 12 h at 37 °C, and then insoluble Lys-type PG was collected by centrifugation at 13,000 × *g* for 10 min. The residue was again washed with DDW five times and kept at −20 °C until use. *B. subtilis* DAP-PG precultured with LB broth plus glucose for 12 h was prepared with the same procedure as *S. aureus* Lys-type PG. The insoluble polymeric *E. coli* DAP-type PG was prepared as follows. The harvested cells were suspended in SDS (final concentration, 8%), boiled at 95 °C for 30 min, and then kept at room temperature for 12 h. The pellet was collected by centrifugation at 20,400 × *g* for 30 min, washed with DDW eight times to remove SDS, and resuspended in 0.1 M Tris-HCl (pH 7.4) containing 10 mM $MgCl_2$. DNase (5 units/ml) was added and incubated for 30 min at 37 °C, and then the pellet was collected after centrifugation at 20,400 × *g* for 30 min at room temperature. The pellet was resuspended with 0.1 M Tris-HCl (pH 7.4) containing 10 mM $CaCl_2$ and then treated with α-amylase (0.1 mg/ml) for 16 h at 37 °C. Subsequently, the residues were treated with Pronase (0.2 mg/ml) for 16 h at 50 °C. The pellet was collected after centrifugation at 20,400 × *g* for 30 min and then washed with DDW three times. Finally, the residues were added to SDS solution (final concentration, 4%) and then incubated at 95 °C for 15 min. The residues were washed with DDW eight times to remove SDS and then kept at −20 °C until use.

Examination of PGRP-SA Binding to Insoluble PGs—To examine the binding specificity of PGs with *Tenebrio* PGRP-SA, the binding assay was performed according to our previously published method (29). Briefly, 1 μg of the recombinant *Tenebrio* PGRP-SA was mixed with 40 μl of a 50% (v/v) suspension of the insoluble Lys-type PGs from *S. aureus* and *M. luteus* and DAP-type PGs from *B. subtilis* and *E. coli* (40 μg) in 50 mM Tris-HCl (pH 7.0) at 4 °C for 12 h with rocking. Unbound PGRP-SA isolated from the supernatant, and bound PGRP-SA recovered from insoluble PGs was analyzed by SDS-PAGE under reducing conditions.

Phenoloxidase (PO) and Amidase Assay—A PO assay was carried out according to a previously published method (32). One unit of PO activity was defined as the amount of enzyme needed to cause a 0.1 increase in absorbance at 520 nm/10-min incubation (A_{520}/10 min). An amidase assay was carried out according to our previously published method (27), and commercially available α-thrombin substrate (*t*-butyloxycarbonyl-benzyl-L-phenylalanyl-L-seryl-L-arginine-4-methyl-coumaryl-7-amide (Boc-Val-Pro-Arg-MCA)) was used.

Antibacterial Activity Assay—Antibacterial activity was assayed after injection of whole bacteria or Lys-type and DAP-type PGs (33). Briefly, bactericidal activities of the hemolymph previously injected with either the soluble Lys-type PG, polymeric DAP-type PG, or lysozyme-treated DAP-type PG (monomeric DAP-type PG) were assayed against *S. aureus* (strain Cowan 1) and *E. coli* (strain K12). These bacteria were harvested in the exponential phase of growth and then suspended in 10 mM sodium phosphate buffer containing 130 mM NaCl (pH 6.0) (buffer A). The collected hemolymph that was obtained after injection was diluted serially with buffer A containing 0.2% bovine serum albumin, and then a portion (10 μl) of the diluted samples was incubated with 1.0×10^6 *S. aureus* cells in 200 μl of insect saline (130 mM NaCl, 5 mM KCl, 1 mM $CaCl_2$) for 60 min at 37 °C. Then the mixtures were diluted 2,000-fold with insect saline, and aliquots of 50 μl were spread on Difco nutrient agar. The plates were incubated for 18 h at 37 °C, and the colony numbers on test and control plates were compared.

Purification of Tenebrio GNBP3, Modular Serine Protease (MSP), SPE-activating Enzyme (SAE), SPE, and Tribolium Spätzle Proteins—The native and recombinant *Tenebrio* proteins, such as GNBP3, MSP, SAE, and SPE and the recombinant *Tribolium castneum*, Spätzle were obtained as described previously (30).

Tenebrio PGRP-SA and PGRP-SC2 Expression Pattern by Injection of S. aureus and E. coli Live Cells—Five μl of cultured *S. aureus* and *E. coli* cells (5.0×10^6) was microinjected into *Tenebrio* larva, and hemolymphs were collected after 30 min, 2 h, 8 h, 12 h, 1 day, 2 days, 3 days, 4 days, and 5 days into 500 μl of cold anti-coagulation buffer. Each sample was used for Western blot analysis with anti-*Tenebrio* PGRP-SA polyclonal antibodies or anti-*Tenebrio* PGRP-SC2 polyclonal antibodies.

Real Time Quantitative PCR Analysis—Total RNA was extracted at the indicated time points with RNAzol reagent for hemocytes (insect blood cells) or fat bodies from *T. molitor* larvae that had been injected with Lys-type PGs, polymeric DAP-type PGs, or lysozyme-treated DAP-type PGs. The first cDNA was synthesized using a first cDNA synthesis kit (Roche Applied Science) according to the manufacturer's instructions. To quantify the AMP gene expression, fluorescence real time quantitative PCR was performed with the dou-

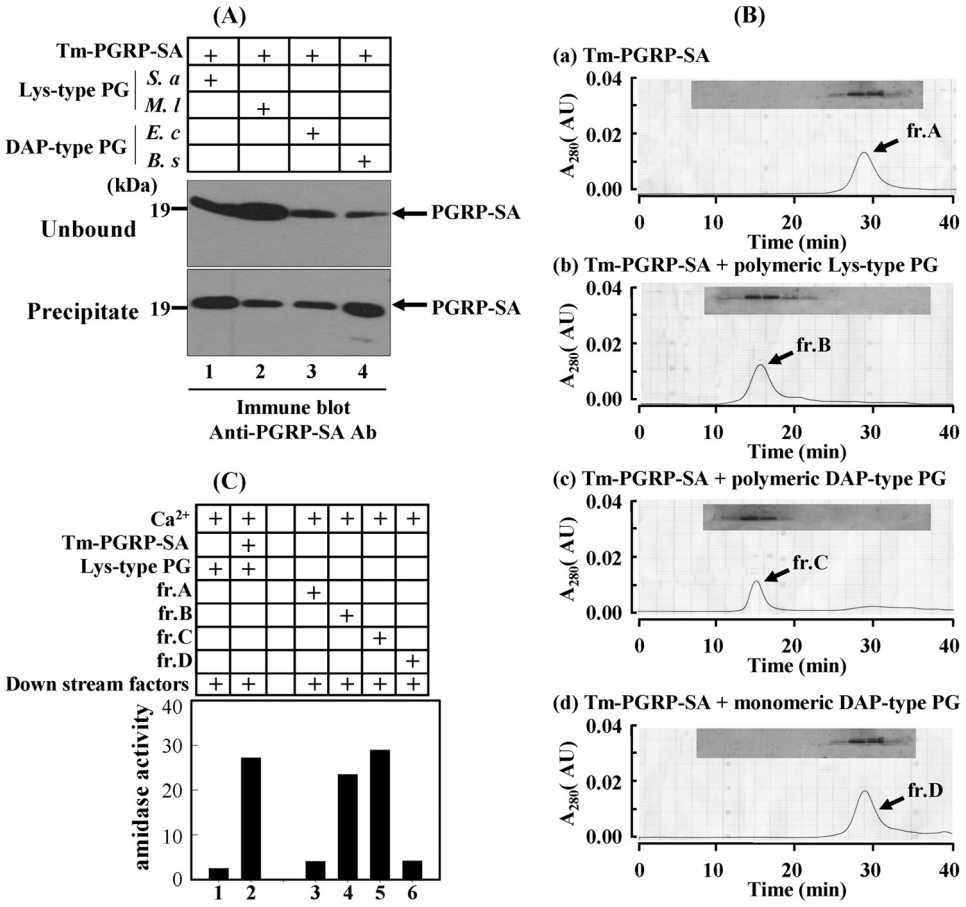

FIGURE 1. **Polymeric DAP-type PG forms a complex with PGRP-SA and induces activation of SPE zymogen.** *A*, the ability of *Tenebrio* PGRP-SA to bind to polymeric Lys-type and DAP-type PGs. *Lanes 1* and 2, *Tenebrio* PGRP-SA with *S. aureus* and *M. luteus* Lys-type PGs, respectively. *Lanes 3* and *4*, PGRP-SA with *E. coli* and *B. subtilis* polymeric DAP-type PGs, respectively. *Tenebrio* PGRP-SA supernatant and precipitate were analyzed by SDS-PAGE. *B*, elution patterns of gel filtration column after loading *Tenebrio* PGRP-SA only (*panel a*), PGRP-SA with polymeric Lys-type PG (*panel b*), PGRP-SA with polymeric DAP-type PG (*panel c*), and PGRP-SA with lysozyme-treated monomeric DAP-type PG (*panel d*). The *boxes* indicate the SDS/PAGE analyses patterns of the fractions after column. *C*, measurement of amidase activity of activated SPE. *Lane 2*, a mixture of Lys-type PG with PGRP-SA and downstream factors (GNBP1, MSP, SAE, and SPE zymogens). *Lanes 3–6* indicate the amidase activities of a mixture of fractions A–D in Fig. 6*B* with downstream factors in the presence of Ca^{2+}. *Tm*, *T. molitor*.

ble-stranded DNA dye, SYBR Green (PerkinElmer Life Sciences). Primer pairs for *tenecin 1* (sense, 5′-ATGAAGCTT ACAATC TTCGCA-3′; antisense, 5′-TTATCTGCAAACG-CAGACCC-3′), *tenecin 2* (sense, 5′-CAGCAAAAC GGA GGATGG T-3′; antisense, 5′-TGC GTT GAA ATC GTG ATC TTG-3′), and the control ribosomal protein L-27A (RPL27A) (sense, 5′-GCATGG CAA ACA CAG AAA GCA TC-3′; antisense, 5′-ATGACA GGT TGG TTA GGC AGG C-3′) were used to detect the target gene transcripts. SYBR Green analysis was performed on an ABI PRISM 7700 system (PE Applied Biosystems) according to the manufacturer's instructions. All of the samples were analyzed in triplicate, and the levels of the detected mRNAs were normalized to control *RPL27A* values. The normalized data were used to quantify the relative levels of a given mRNA according to the ΔC_t analysis (15).

RESULTS

Polymeric DAP-type PG Binds PGRP-SA and Activates the Downstream Proteases Like Lys-type PG—Since we reported that DAP-type PG can bind to *Tenebrio* PGRP-SA and induce pro-PO activation *in vitro* (28) and that PGRP-SA-mediated proteolytic cascade activation results in melanin synthesis (34), we have wondered whether polymeric DAP-type PGN could induce the PGRP-SA-mediated Toll signaling cascade similarly to Lys-type PG. To examine how DAP-type PGs modulate insect innate immune responses, it is necessary to purify homogeneous polymeric DAP-type PGs. We purified DAP-type PGs from *E. coli* and *B. subtilis*, and then their amino acid compositions were analyzed to determine their purities. Molar ratios of amino acids of *E. coli* and *B. subtilis* DAP-type PGs were matched with the expected ratio (Ala:Glu:DAP = 2:1:1, supplemental Table S1), indicating that our polymeric DAP-type PGs are pure and do not contaminate with other proteins. When insoluble Lys-type PGs from *S. aureus* and *M. luteus* or insoluble DAP-type PGs from *B. subtilis* and *E. coli* were incubated with *Tenebrio* recombinant PGRP-SA, PGRP-SA bound to both DAP-type PGs (Fig. 1*A*, *lanes 3* and *4*) and Lys-type PGs (*lanes 1* and *2*), indicating that DAP-type PGs were recognized by *Tenebrio* PGRP-SA. Previously, we reported that complex formation between *Tenebrio* PGRP-SA and polymeric Lys-type PG is essential for sensing polymeric Lys-type PG, leading to activation of the *Tenebrio* pro-PO cascade (29). When we loaded a mixture of polymeric DAP-type PG and PGRP-SA on the gel filtration column, a complex between DAP-type PG and PGRP-SA was generated (Fig. 1*B*, *panels b* and *c*). Under the same conditions, lysozyme-treated DAP-type PG, monomeric form, did not form a complex (Fig. 1*B*, *panel d*). These results suggest that polymeric DAP-type PG also induces clustering of *Tenebrio* PGRP-SA on polymeric DAP-type PG. If polymeric DAP-type PG is recognized by PGRP-SA, we hypothesized that the downstream factors of the polymeric DAP-type PG recognition signal pathway will be also the same as those of the Lys-type PG-dependent Toll pathway. To confirm this possibility, we examined amidase activity derived from activated SPE after incubation of the DAP-type PG·PGRP-SA complex with downstream factors including GNBP1 and three SP zymogens: pro-MSP, pro-SAE, and pro-SPE, in the presence of calcium ions (Fig. 1*C*). As expected, the polymeric DAP-type PG·PGRP-SA complex induced strong amidase activity against the SPE-specific fluorescence synthetic substrate (*column 5*). Under the same conditions, the Lys-type PG·PGRP-SA complex also

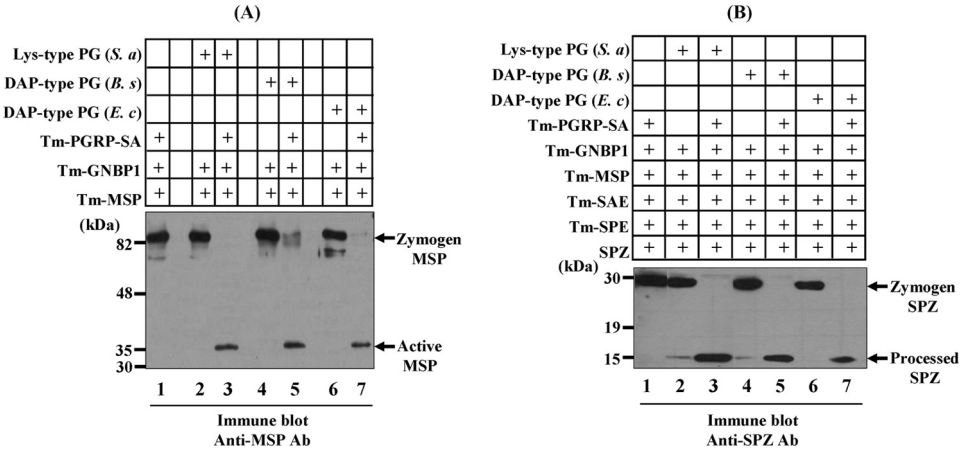

FIGURE 2. ***In vitro* reconstitution experiments for the activation of pro-MSP and processing of pro-Spätzle by polymeric DAP-type PG.** *A*, mixture of purified *Tenebrio* PGRP-SA, GNBP1, and MSP zymogen in the presence of *S. aureus* Lys-type PG (*lanes 2* and *3*), *B. subtilis* polymeric DAP-type PG (*lanes 4* and *5*), and *E. coli* DAP-type PG (*lanes 6* and *7*) were incubated for 60 min and then analyzed by Western blotting with an anti-MSP antibody. The 82-kDa pro-MSP and the 35-kDa activated MSP are indicated with *arrows*. In the absence of PGRP-SA, pro-MSP was not cleaved (*lanes 2*, *4*, and *6*). *B*, mixture of *Tenebrio* PGRP-SA, GNBP1, MSP, SAE, SPE zymogens, and pro-Spätzle (*SPZ*) in the presence of *S. aureus* Lys-type PG (*lanes 2* and *3*), *B. subtilis* polymeric DAP-type PG (*lanes 4* and *5*), and *E. coli* DAP-type PG (*lanes 6* and *7*) were incubated for 60 min and then analyzed by Western blotting with an affinity-purified anti-SPZ antibody. The 30-kDa pro-SPZ and the 12-kDa processed SPZ are indicated with *arrows*. As a control, when eight components, such as Lys-type PG·PGRP-SA·GNBP1·MSP·SAE·SPE·Spätzle, were incubated together, the cleaved 12-kDa SPZ was generated (*lane 3*). In the absence of PGRP-SA, pro-SPZ was not converted to the processed SPZ (*lanes 2, 4, and 6*). *Tm*, *T. molitor*; *Ab*, antibody; *S. a*, *S. aureus*; *B. s*, *B. subtilis*; *E. c*, *E. coli*.

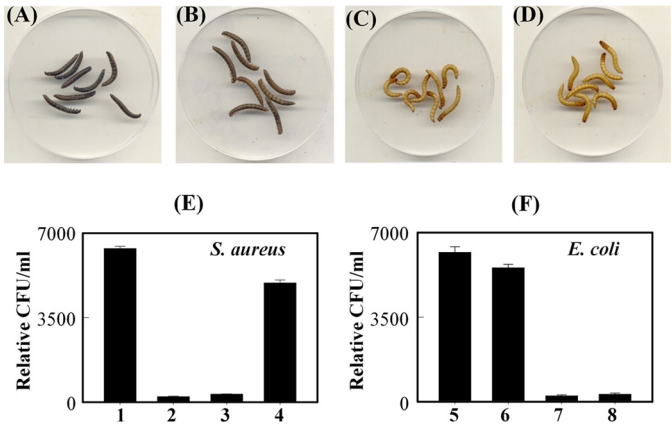

FIGURE 3. **Polymeric DAP-type PG induces melanin and AMP synthesis.** One hundred nanograms of Lys-type PG (*A*), polymeric DAP-type PG (*B*), or lysozyme-treated DAP-type PG (*C*) was injected into ten *Tenebrio* larvae, respectively. Four μl of insect saline was injected as a control (*D*). Within 18 h, the appearance of melanin pigment was examined. Antibacterial activities after injection of PGs (50 ng) are shown against *S. aureus* (*E*) and *E. coli* (*F*), respectively. *Columns 1* and *5*, *columns 2* and *6*, *columns 3* and *7*, and *columns 4* and *8* are injected with insect saline (4 μl), Lys-type PG (50 ng), polymeric DAP-type PG (50 ng), and lysozyme-treated DAP-type PG (50 ng), respectively. After 12 h, hemolymph was collected from each group, and the bactericidal effects were estimated against *S. aureus* and *E. coli*.

induced strong amidase activity (*column 4*), but monomeric DAP-type PG did not induce this activity (*column 6*). These results strongly support that the polymeric DAP-type PG recognition signal is transferred by a PGRP-SA·GNBP1-mediated three-step proteolytic cascade similarly to Lys-type PG.

Polymeric DAP-type PG Induces pro-Spätzle Processing via a PGRP-SA·GNBP1 Complex-mediated Three-step Proteolytic Cascade—If polymeric DAP-type PG also uses the *Tenebrio* Toll pathway for the induction of innate immune responses, we expected the possibility that polymeric DAP-type PG also induces pro-Spätzle processing via a three-step proteolytic cascade. Initially, as a positive control, when Lys-type PG was incubated with PGRP-SA, GNBP1, and MSP zymogen, the active form of MSP was generated as described previously (Fig. 2*A*, *lane 3*). Under the same conditions, when two polymeric DAP-type PGs purified from *B. subtilis* and *E. coli* were incubated with PGRP-SA, GNBP1, and MSP zymogen in the presence of calcium ion, MSP activation was clearly observed (Fig. 2*A*, *lanes 5* and *7*), reconfirming that polymeric DAP-type PGs can induce activation of MSP zymogen to the active form of MSP via the PGRP-SA·GNBP1 complex. If the polymeric DAP-type PG recognition signal can convert MSP zymogen to its active form, pro-Spätzle processing should also occur in *in vitro* reconstitution experiments. As a positive control, Lys-type PG clearly induced pro-Spätzle processing when six components, PGRP-SA, GNBP1, MSP, SAE, SPE, and pro-Spätzle, were co-incubated in the presence of Lys-type PG and calcium ions (Fig. 2*B*, *lane 3*). Under the same conditions, when polymeric Lys-type PG was replaced with polymeric DAP-type PGs, pro-Spätzle was clearly converted to the processed Spätzle form (*lanes 5* and *7*). These results suggest that the polymeric DAP-type PG recognition signal also uses the same components that are involved in the Lys-type PG-dependent Toll signaling cascade.

Polymeric DAP-type PG Recognition Mechanism in Tenebrio Larvae Is Different from That of Drosophila Adults—To examine the effects of polymeric DAP-type PG *in vivo*, polymeric and lysozyme-treated DAP-type PGs were injected into *Tenebrio* larvae (Fig. 3). Polymeric *E. coli* DAP-type PG, but not lysozyme-treated DAP-type PG, strongly induced melanin synthesis in *Tenebrio* larvae (Fig. 3, *B* and *C*). As a control, polymeric Lys-type PG also induced melanin synthesis (Fig. 3*A*). Similar to these *in vivo* results, both polymeric DAP-type and Lys-type PGs showed strong PO activities, but lysozyme-treated DAP-type PG did not show PO activity *in vitro* (supplemental Fig. S1). These results demonstrate that polymeric DAP-type PG, but not lysozyme-treated DAP-type PG, can activate the pro-PO cascade, leading to melanin synthesis similarly to polymeric Lys-type PGs. Next, inducible AMP production by injection of polymeric- and lysozyme-treated DAP-type PGs were estimated in *Tenebrio* larvae (Fig. 3, *E* and *F*). Polymeric DAP-type PG showed bactericidal activities against both *S. aureus* and *E. coli* (*columns 3* and *7*), but lysozyme-treated DAP-type PG only showed bactericidal activity against *E. coli* (*column 8*). Recently, we demonstrated that the activation of Lys-type PG and the β-1,3-glucan-dependent *Tenebrio* Toll signaling pathway induces two AMPs, tenecin 1 and tenecin 2,

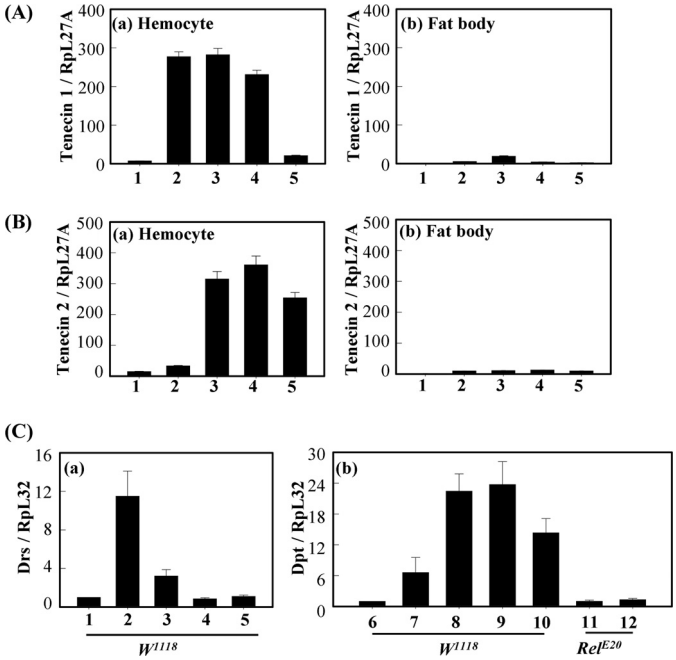

FIGURE 4. **The mRNA expression levels of *Tenebrio* and *Drosophila* AMPs by challenge of DAP-type PGs.** *A* and *B* represent the mRNA levels of tenecin 1 and 2 in *Tenebrio* hemocytes (*panel a*) and fat bodies (*panel b*), respectively. *C* represents the mRNA levels of *Drosophila* drosomycin (*Drs*, *panel a*) and diptericin (*Dpt*, *panel b*) in w^{1118} and Rel^{E20} strains. Shown are insect saline (*column 1*), *S. aureus* Lys-type PG (*column 2*), *E. coli* polymeric DAP-type PG (*column 3*), *B. subtilis* polymeric DAP-type PG (*column 4*), and lysozyme-treated *E. coli* DAP-type PG (*column 5*). *Columns 6–10* represent the same injections as those in *columns 1–5* in Fig. 4*C* (*panel a*), respectively. *Columns 11* and *12* represent the same injections as those in *columns 1* and *3* in Fig. 4*C* (*panel a*), respectively. The mRNA levels of tenecin 1 or 2 relative to that of insect saline-injected *T. molitor* larvae at 12 h after injection are shown. *Error bars*, means ± S.D. ($p \leq 0.05$) of three independent experiments.

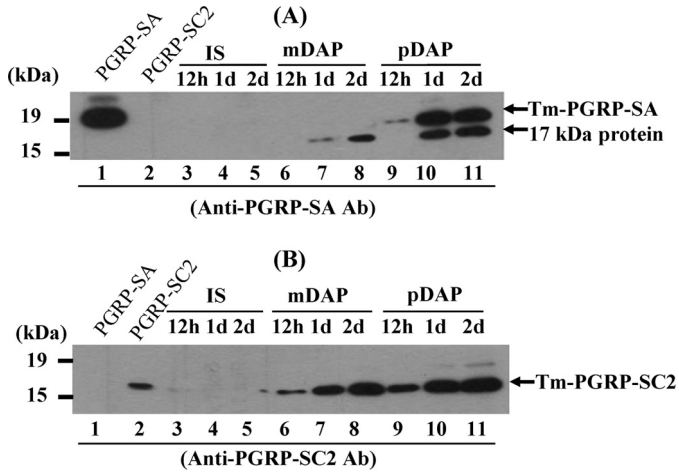

FIGURE 5. **The amounts of *Tenebrio* PGRP-SA and 17-kDa protein in the hemolymph increased after injection of polymeric Lys-type and DAP-type PGs.** *A* and *B* represent Western blot analysis using anti-PGRP-SA and anti-PGRP-SC2 antibodies, respectively. *Lanes 1* and *2* indicate the purified PGRP-SA (500 ng) and the purified PGRP-SC2 (500 ng), respectively. *Lanes 3-5*, *lanes 6–8*, and *lanes 9–11* represent the injection of insect saline (*IS*), monomeric DAP-type PG (*mDAP*), and polymeric DAP-type PG (*pDAP*) after 12 h, 1 days (*1d*), and 2 days (*2d*), respectively. At the indicated times, hemolymph was collected, and then a portion (40 μg of protein) of each sample was analyzed by immunoblotting using affinity-purified anti-*Tenebrio* PGRP-SA and PGRP-SC2 antibodies. *Ab*, antibody.

which were very similar to *Drosophil*a defensin and diptericin, respectively (31, 35). Diptericin and tenecin 2 are effective against Gram-negative bacteria, whereas defensin and tenecin 1 are active against Gram-positive bacteria and fungi. Because antibacterial activities were shown after injection of DAP-type PGs, we carried out real time quantitative PCR analysis on mRNA fractions that were obtained from the fat bodies or hemocytes of the *Tenebrio* larva, which were collected 12 h after injection of polymeric- and lysozyme-treated DAP-type PGs. As expected, tenecin 1 was dramatically induced in *Tenebrio* hemocytes by injection of polymeric DAP-type PGs (Fig. 4*A*, *columns 3* and *4*) similarly to Lys-type PG (*column 2*) but only slightly induced in fat bodies. However, injection of lysozyme-treated DAP-type PG did not induce tenecin 1 from hemocytes and fat bodies (Fig. 4*A*, *column 5*). Tenecin 2 expression was observed after the injection of polymeric DAP-type and lysozyme-treated DAP-type PGs (Fig. 4*B*, *columns 3–5*), but not Lys-type PG (column 2), into hemocytes. These results demonstrate that polymeric DAP-type PGs induce PO activation in hemolymph and tenecin 1 in hemocytes, suggesting that polymeric DAP-type PG activates the *Tenebrio* Toll signaling pathway. To confirm induced *Drosophila* AMPs after injection of polymeric- and lysozyme-treated monomeric DAP-type PGs, we performed real time PCR analysis using w^{1118} control flies and Imd pathway mutant flies (Rel^{E20}) (Fig. 4*C*). As reported previously (3, 4), polymeric Lys-type PG induced expression of the drosomycin gene in w^{1118} control flies (Fig. 4*C*, *column 2*), which is predominantly induced after activation of the Toll signaling pathway. As expected, polymeric DAP-type PGs only slightly induce drosomycin gene expression in w^{1118} control flies (Fig. 4*C*, *columns 3* and *4*). However, polymeric DAP-type PGs strongly induced diptericin gene expression in w^{1118} control flies, and the diptericin gene is known to be induced after Imd pathway activation via the PGRP-LC receptor (Fig. 4*C*, *columns 8* and *9*). Under the same conditions, diptericin was not induced by injection of polymeric DAP-type PG in Imd pathway mutant flies (Fig. 4*C*, *column 12*). Taken together, these results suggest that AMP production patterns by injection of polymeric DAP-type PGs in *Tenebrio* larvae and *Drosophila* adults are different, indicating that polymeric DAP-type PG-mediated Toll signaling activation in *Tenebrio* larvae is a characteristic response.

Injection of Polymeric DAP-type PG Induces the Expression of Tenebrio PGRP-SA and 17-kDa Protein Simultaneously in the Hemolymph—Because monomeric DAP-type PG induced AMP activity against *E. coli* but not *S. aureus* in *Tenebrio* larvae that might be due to tenecin 2, we tried to identify a new protein regulating the DAP-type PG-mediated immune response in *Tenebrio* hemolymph. Among our trials, we found that our PGRP-SA antibody cross-reacted with an unidentified 17-kDa protein and that both the unidentified 17-kDa protein and 19-kDa *Tenebrio* PGRP-SA were strongly induced 24 h after polymeric DAP-type PG injection (Fig. 5*A*, *lanes 10* and *11*). The unidentified 17-kDa protein and PGRP-SA were also induced by injection of *S. aureus* cells, *E. coli* cells or purified polymeric Lys-type PG (supplemental Fig. S2), but PGRP-SA was not induced by injection of lysozyme-treated DAP-type PG (Fig. 5*A*, *lanes 7* and *8*). Interestingly, the 17-kDa protein was still induced by injection of lysozyme-treated monomeric DAP-type PG (*lanes 7* and *8*).

```
Tm-PGRP-SC2 : MFFIILLISLLPYLAQC-----------SCPTIISRSEWGARAPKSVKNLSQNPPPFVVVHHSDTPP-CSTLSSCKSRVKNIQN :  72
Dm-PGRP-SC2 : MANKALVLLAVLFCAQAVLG----------VTIVSKSEWGGRSATSKTSLANYLS-YAVIHHTAGNY-CSTKAACITQLQNIQT :  72
Dm-PGRP-LB  : MQQANLGDGVATARL-------------------LSRSDWGARLPKSVEHFQ-GPAPYVIIHHSYMPAVCYSTPDCMKSMRDMQD :  65
Dm-PGRP-SB1 : MNTSTAISLVAALVLCCLALSANA-------LQIEPRSSWGAASARSPSRIS-GAVDYVIIHHSDNPNGCSTSEQCKRMIKNIQS :  77
Tm-PGRP-SA  : MLLATIARGVYQISA------LSGSTIPRICPEIISRTRWGARTP-LEVDYSLIPIENVVVHHTVTHT-CDSESECATLLRNVQN :  77

Tm-PGRP-SC2 : YHMDNRGWQDIGYNFLIGGDGNVYEGRGWGIWGAHVPRYNSKSIGICVIGDFQNEKPPTTQLNTLESLISCAKEKGYIQTNYHLI : 157
Dm-PGRP-SC2 : YHMDSLGWADIGYNFLIGGDGNVYEGRGWNVMGAHATNWNSKSIGISFLGNYNTNTLTSAQITAAKGLLSDAVSRGQIVSGYILY : 157
Dm-PGRP-LB  : FHQLERGWNDIGYSFGIGGDGMIYTGRGFNVIGAHAPKYNDKSVGIVLIGDWRTELPPKQMLDAAKNLIAFGVFKGYIDPAYKLL : 150
Dm-PGRP-SB1 : DHKGRRNFSDIGYNFIVAGDGKVYEGRGFGLQGSHAPNYNRKSIGIVFIGNFERSAPSAQMLQNAKDLIELAKQRGYLKDNYTLF : 162
Tm-PGRP-SA  : FHMENLEFHDIGYNFLVAGDGQIYEGAGWHKVGAHTRGYNTRSLGLAFIGNFTSQLPVQKQLKVAKDFLQCGVELGELSKNYKLF : 162

Tm-PGRP-SC2 : GHRQGSQTTCPGNALFNEIKTWPNFDSNVRP-------------------------------- : 188
Dm-PGRP-SC2 : GHRQVGSTECPGTNIWNEIRTWSNWKA---------------------------------- : 184
Dm-PGRP-LB  : GHRQVRDTECPGGRLFAEISSWPHFTHINDTEGVSSTTAPVVPHVHPQAAAPQKPHQSPPAAPKV: 215
Dm-PGRP-SB1 : GHRQTKATSCPGDALYNEIKTWPHWRQN-------------------------------- : 190
Tm-PGRP-SA  : GARQVSSTSSPGLKLYRELQDWPHFTRSPPK-------------------------------- : 193
```

FIGURE 6. **Multiple amino acid sequence alignment between *Tenebrio* PGRP-SC2 and *Drosophila* PGRP family members.** Three residues conserved from T7 lysozymes are shown with *boxes*. Two residues (His and Cys residues) that were not conserved with *Tenebrio* PGRP-SA are shown in *boxes* marked with *circles*. The GenBank™ or Swissprot accession numbers for the sequences used are as follows: *T. molitor* (*Tm*) PGRP-SA, BAE78510.1; and *D. melanogaster* (*Dm*) PGRP-SC2, Q9V4X; PGRP-LB, Q9VGN3; PGRP-SB1, Q9VV97. The determined partial amino acid sequences are indicated by *underlining*.

The Inducible 17-kDa Protein Is DAP-type PG-scavenging Tenebrio PGRP-SC2—To characterize the 17-kDa protein, we determined the partial amino acid sequences of the 17-kDa protein after purification. The obtained partial sequences showed high homology with those of *Drosophila* PGRP-SC2 (data not shown). When we cloned the cDNA of this 17-kDa protein based on the partial amino acid sequences, the 17-kDa protein showed 46 and 45% sequence homologies with *Drosophila* PGRP-SC2 and *Tenebrio* PGRP-SA, respectively (Fig. 6). To examine the biological functions of *Tenebrio* PGRP-SC2, we expressed and purified this protein using the insect Sf9 cell expression system and raised polyclonal antibodies specifically recognizing *Tenebrio* PGRP-SC2 but not *Tenebrio* PGRP-SA (Fig. 5*B*). We reconfirmed using anti-PGRP-SC2-specific antibodies that PGRP-SC2 was specifically induced by injection of monomeric DAP-type PG and polymeric Lys- and DAP-type PGs into *Tenebrio* larvae (Fig. 5*B* and supplemental Fig. S3). In addition, because cysteine residues of *Drosophila* PGRP-SC2 and PGRP-LB that are known to be essential residues for *N*-acetylmuramyl-L-alanine amidase activity are conserved in *Tenebrio* PGRP-SC2 (Fig. 6), we assumed that *Tenebrio* PGRP-SC2 also has *N*-acetylmuramyl-L-alanine amidase activity against PGs. As expected, recombinant *Tenebrio* PGRP-SC2 showed strong amidase activities against DAP-type PG (Fig. 7*A*), but this protein showed weak amidase activity against Lys-type PG (Fig. 7*B*). When the cysteine residue of *Tenebrio* PGRP-SC2 was replaced with a serine residue, amidase activity of the PGRP-SC2 C167S mutant was completely abolished (Fig. 7*A*). Furthermore, to confirm the cleavage site of DAP-type PG by PGRP-SC2, we compared the HPLC profiles of lysozyme-treated DAP-type PG and monomeric DAP-type PG cleaved with PGRP-SC2 (supplemental Fig. S4). The profile of monomeric DAP-type PG shows three peaks (supplemental Fig. S4*B*), which showed no positive signals by Edman degradation (data not shown), indicating that the lactylamide bond between the glycan backbone and the stem peptides of DAP-type PG was not cleaved. In contrast, two peaks were eluted when the major peak of fraction (B) was incubated with *Tenebrio* PGRP-SC2 (supplemental Fig. S4*C*). The N-terminal sequence of the generated peptide by treatment of PGRP-SC2 on monomeric DAP-type PG was determined and found to be Ala-Glu, indicating that lactylamide bond of DAP-type PG was cleaved by PGRP-SC2. Taken together, these results suggest that noncatalytic *Tenebrio* PGRP-SA and catalytic PGRP-SC2 are simultaneously induced by injection of polymeric DAP-type PG.

Tenebrio PGRP-SC2-treated Polymeric DAP-type PG Cannot Induce AMP Production—Because *Tenebrio* PGRP-SC2 specifically cleaved polymeric DAP-type PGs, we expected that injection of PGRP-SC2-treated polymeric DAP-type PG cannot induce AMP production. As expected, tenecin 1 induction was largely abolished by injection of PGRP-SC2-treated DAP-type PG into *Tenebrio* larvae (Fig. 7*C*, *column 3*). Under the same conditions, PGRP-SC2-treated Lys-type PG produced no change in tenecin 1 induction (*column 5*). In addition, tenecin 2 induced by injection of polymeric DAP-type PG (*column 2*) was also abolished by injection of PGRP-SC2-treated polymeric DAP-type PG (*column 3*). These results demonstrate that PGRP-SC2 protein might function as a DAP-type PG scavenger by degradation of DAP-type PGs, leading to the down-regulation of innate immune response *in vivo*.

DISCUSSION

In this study, we have described the first biochemical evidence of how the polymeric DAP-type PG recognition signal is transferred to Spätzle, leading to AMP production (tenecin 1 and 2) in *Tenebrio* larvae, which are distinct from *Drosophila* adults. As we previously described, the PGRP-SA·GNBP1·MSP·SAE·SPE·Spätzle unit is an essential unit that triggers the polymeric Lys-type PG recognition signaling pathway in response to Gram-positive bacteria, and this unit is shared with polymeric DAP-type PG recognition and the resulting response to Gram-negative and certain Gram-positive bacteria (*Bacillus* species). Additionally, the MSP/SAE/SPE/Spätzle proteolytic cascade is also used in β-1,3-glucan-GNBP3 recognition signaling in response to fungal infection. Moreover, the MSP·SAE·SPE cascade activates pro-PO for melanization. Therefore, coleopteran *Tenebrio* larvae initiate immune defense using the

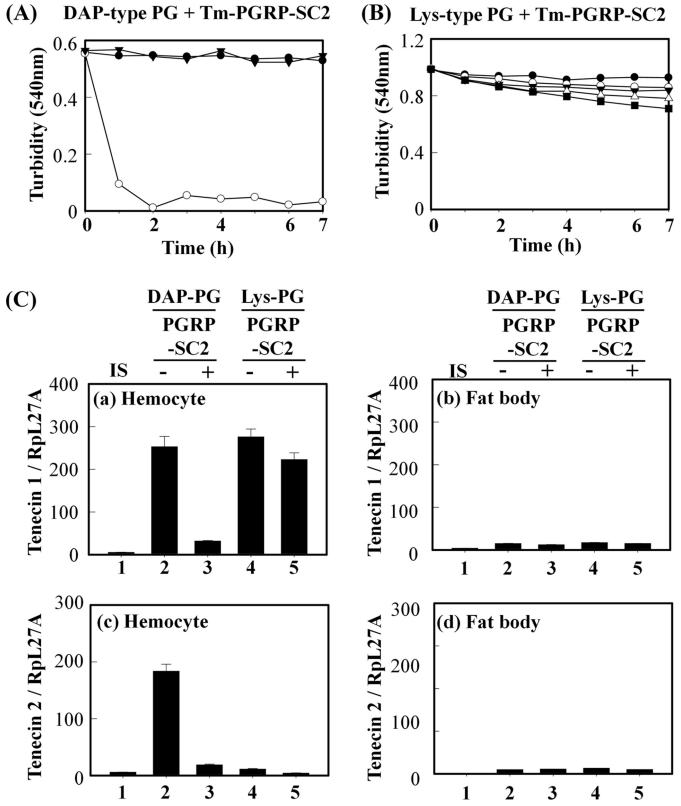

FIGURE 7. **Catalytic *Tenebrio* PGRP-SC2 functions as a scavenger for polymeric DAP-type PG.** *A*, kinetics of polymeric DAP-type PG degradation by *Tenebrio* PGRP-SC2. Insoluble polymeric DAP-type PG (1 mg/ml) was incubated with recombinant wild type PGRP-SC (5 μg/ml, ○), PGRP-SC2 (C167S)-mutant (5 μg/ml, ●), and the absence of protein (▼) in PBS (pH 7.2). *B*, insoluble polymeric *S. aureus* Lys-type PG (1 mg/ml) was incubated with different concentrations of *Tenebrio* recombinant PGRP-SC2, such as 0 (●), 5 (○), 10 (▼), 20 (△), and 40 (■) μg/ml. Enzymatic activity was recorded as the optical clearance of the solution at 540 nm. *C*, tenecin 1 (*panels a* and *b*) and tenecin 2 (*panels c* and *d*) expression were examined by injection of *Tenebrio* PGRP-SC2-treated polymeric DAP-type PG in the hemocytes (*panels a* and *c*) and fat bodies (*panels b* and *d*). *Tenebrio* larvae were challenged with insect saline (*IS*, *column 1*), polymeric DAP-type PG (12.5 μg/ml, *column 2*), *Tenebrio* PGRP-SC2-treated polymeric DAP-type PG (12.5 μg/ml, *column 3*), polymeric Lys-type PG only (12.5 μg/ml, *column 4*), and *Tenebrio* PGRP-SC2-treated polymeric Lys-type PG (12.5 μg/ml, *column 5*). Total RNA was isolated at 12 h after challenge with PGs. The mRNA levels of tenecin 1 and 2 relative to that of insect saline-injected *T. molitor* (*Tm*) larvae at 12 h after injection are shown. *Error bars*, means ± S.D. ($p \leq 0.05$) of three independent experiments.

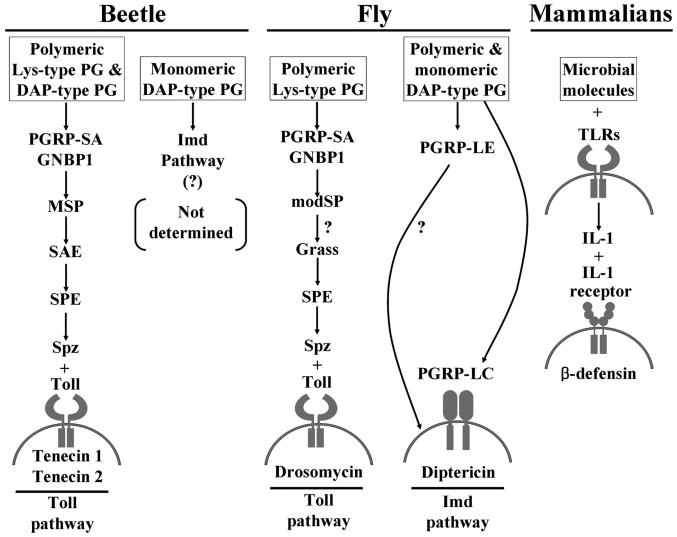

FIGURE 8. **Parallel comparison for the induction of AMPs after recognition of microbial molecules in beetle, fly, and mammalian.** The Lys-type PG-dependent *Tenebrio* Toll signaling pathway was previously reported by our group (30). *Drosophila* Toll and Imd pathways were reviewed by Lemaitre and Hoffmann (2). The mammalian β-defensin induction pathway was reported by Ganz and co-workers (40). Namely, mammalian Toll-like receptor (*TLR*)-dependent expression of AMPs in keratinocytes is induced by an activated cytokine, IL-1, which is directly inducible by TLRs of monocytes and macrophages (41). A *plus sign* in mammalian β-defensin induction pathway means the interaction between ligand and its receptor.

Toll-activating proteolytic signaling pathway by sensing the PGs of invading pathogens (Fig. 8). These observations were also reported for a silkworm larvae, *B. mori*, in which PGs obtained from Gram-positive and Gram-negative bacteria and β-1,3-glucan from fungi activate pro-PO (36, 37), although the molecular mechanisms of PG recognition signals were not suggested. Also, the pro-PO cascade in *B. mori* hemolymph was stimulated by high molecular weight insoluble PG but not by lysozyme-digested PG (37). Based on our biochemical data, we suppose that *B. mori* larvae might use the same PG recognition signal pathways for their host defenses as *Tenebrio* larvae.

Our data demonstrate that polymeric DAP-type PG-mediated Toll signaling is unique to the beetle and does not occur in the fly, suggesting a different method of linking polymeric DAP-type PG recognition and innate immune responses in two insect species. The reason for these diverse recognition mechanisms for polymeric DAP-type PG might be developmental differences in two species. One possible explanation is that *Tenebrio* PGRP-SA can recognize both Lys-type- and DAP-type PG as shown in our *in vitro* binding assay (28). However, *Drosophila* PGRP-SA was reported to recognize Lys-type PG preferentially rather than DAP-type PG (38). *Drosophila* PGRP-LE or LC is known to recognize DAP-type PG preferentially (16, 38). These properties will be applied on the larval and adult stages in two insects, leading to *Tenebrio* larvae recognizing polymeric Lys-type and DAP-type PG simultaneously. Namely, *Tenebrio* larvae first recognize polymeric DAP-type PG via PGRP-SA·GNBP1 complex, and then generated monomeric DAP-type PG by hemolymph lysozyme will be recognized by another PGRP molecule, such as *Drosophila* PGRP-LE- or LC-like homologue, leading to the activation of Imd signaling pathway. In contrast, *Drosophila* adults may recognize DAP-type and Lys-type PG differently via different PGRP molecules.

We also provide evidence that monomeric DAP-type PG generated by lysozyme digestion induces tenecin 2 and PGRP-SC2. Probably, polymeric DAP-type PGs of Gram-negative bacteria and Gram-positive *Bacillus* species were degraded by soluble lysozyme in the hemolymph, and the resulting monomeric DAP-type PGs should be recognized by the *Drosophila* PGRP-LE homologue of *T. molitor* or an unidentified novel receptor. Then the monomeric DAP-type PG recognition signal will be transferred to downstream molecules, leading to induction of *Drosophila* diptericin-like AMP tenecin 2 in the hemolymph. Until now, although we tried to clone a *Drosophila* PGRP-LE homologue in *Tenebrio* cDNA library, our efforts to find this gene proved unsuccessful. We also show the function of the *Tenebrio* PGRP-SC2, a catalytic PGRP family protein that functions as a DAP-type PG scavenger. PGRP-SC2 is the

N-acetylmuramyl-L-alanine amidase specific for DAP-type PG and plays roles in negative feedback regulation of immune responses induced by not only polymeric DAP-type PG but also monomeric DAP-type PG. Consistent with this function, PGRP-SC2 was induced by injection of lysozyme-treated DAP-type PG as well as polymeric DAP-type PG (Fig. 5). The production of PGRP-SC2 might be activated under both the Toll signaling pathway and the unidentified monomeric DAP-PG-activated signaling pathway. Recently, we reported three serpins that specifically inactivate MSP, SAE, and SPE, respectively, and two of the three serpins are induced by Toll pathway activation (39). PGRP-SC2 down-regulates the Toll signaling pathway in collaboration with these serpins. On the other hand, the induction of PGRP-SA by polymeric Lys-type and DAP-type PG, which appears to be caused by Toll activation, might function to prepare innate immune responses against the second infection.

In summary, our biochemical studies shed further light on the biological diversity of the molecular mechanisms of polymeric DAP-type PG recognition signals in insects. Our work supports a model in which polymeric Lys- and DAP-type PG recognition complexes activate three different *Tenebrio* SPs zymogens sequentially. This three-step proteolytic cascade-dependent processing of the extracellular protein pro-Spätzle and then the binding of the processed Spätzle to the Toll receptor are required for the induction of AMPs expression in *Tenebrio* larvae. A greater understanding of DAP-type and Lys-type binding abilities of *Tenebrio* PGRP-SA will also facilitate the development of a novel kit to rapidly and sensitively detect Gram-positive and Gram-negative bacterial PGs in blood and food products.

REFERENCES

1. Schleifer, K. H., and Kandler, O. (1972) *Bacteriol. Rev.* **36,** 407–477
2. Lemaitre, B., and Hoffmann, J. (2007) *Annu. Rev. Immunol.* **25,** 697–743
3. Georgel, P., Naitza, S., Kappler, C., Ferrandon, D., Zachary, D., Swimmer, C., Kopczynski, C., Duyk, G., Reichhart, J. M., and Hoffmann, J. A. (2001) *Dev. Cell* **1,** 503–514
4. Lemaitre, B., Nicolas, E., Michaut, L., Reichhart, J. M., and Hoffmann, J. A. (1996) *Cell* **86,** 973–983
5. Hedengren, M., Asling, B., Dushay, M. S., Ando, I., Ekengren, S., Wihlborg, M., and Hultmark, D. (1999) *Mol. Cell* **4,** 827–837
6. Kang, D., Liu, G., Lundström, A., Gelius, E., and Steiner, H. (1998) *Proc. Natl. Acad. Sci. U.S.A.* **95,** 10078–10082
7. Yoshida, H., Kinoshita, K., and Ashida, M. (1996) *J. Biol. Chem.* **271,** 13854–13860
8. Liu, C., Xu, Z., Gupta, D., and Dziarski, R. (2001) *J. Biol. Chem.* **276,** 34686–34694
9. Dziarski, R., Platt, K. A., Gelius, E., Steiner, H., and Gupta, D. (2003) *Blood* **102,** 689–697
10. Mellroth, P., Karlsson, J., and Steiner, H. (2003) *J. Biol. Chem.* **278,** 7059–7064
11. Levashina, E. A., Langley, E., Green, C., Gubb, D., Ashburner, M., Hoffmann, J. A., and Reichhart, J. M. (1999) *Science* **285,** 1917–1919
12. El Chamy, L., Leclerc, V., Caldelari, I., and Reichhart, J. M. (2008) *Nat. Immunol.* **9,** 1165–1170
13. Belvin, M. P., and Anderson, K. V. (1996) *Annu. Rev. Cell Dev. Biol.* **12,** 393–416
14. Mishima, Y., Quintin, J., Aimanianda, V., Kellenberger, C., Coste, F., Clavaud, C., Hetru, C., Hoffmann, J. A., Latgé, J. P., Ferrandon, D., and Rousselsel, A. (2009) *J. Biol. Chem.* **284,** 28687–28697
15. Leulier, F., Parquet, C., Pili-Floury, S., Ryu, J. H., Caroff, M., Lee, W. J., Mengin-Lecreulx, D., and Lemaitre, B. (2003) *Nat. Immunol.* **4,** 478–484
16. Takehana, A., Katsuyama, T., Yano, T., Oshima, Y., Takada, H., Aigaki, T., and Kurata, S. (2002) *Proc. Natl. Acad. Sci. U.S.A.* **99,** 13705–13710
17. Royet, J., Reichhart, J. M., and Hoffmann, J. A. (2005) *Curr. Opin. Immunol.* **17,** 11–17
18. Cherry, S., and Silverman, N. (2006) *Nat. Immunol.* **7,** 911–917
19. Stenbak, C. R., Ryu, J. H., Leulier, F., Pili-Floury, S., Parquet, C., Hervé, M., Chaput, C., Boneca, I. G., Lee, W. J., Lemaitre, B., and Mengin-Lecreulx, D. (2004) *J. Immunol.* **173,** 7339–7348
20. Jang, I. H., Chosa, N., Kim, S. H., Nam, H. J., Lemaitre, B., Ochiai, M., Kambris, Z., Brun, S., Hashimoto, C., Ashida, M., Brey, P. T., and Lee, W. J. (2006) *Dev. Cell* **10,** 45–55
21. Ligoxygakis, P., Pelte, N., Hoffmann, J. A., and Reichhart, J. M. (2002) *Science* **297,** 114–116
22. Kambris, Z., Brun, S., Jang, I. H., Nam, H. J., Romeo, Y., Takahashi, K., Lee, W. J., Ueda, R., and Lemaitre, B. (2006) *Curr. Biol.* **16,** 808–813
23. Buchon, N., Poidevin, M., Kwon, H. M., Guillou, A., Sottas, V., Lee, B. L., and Lemaitre, B. (2009) *Proc. Natl. Acad. Sci. U.S.A.* **106,** 12442–12447
24. Hoffmann, J. A. (2003) *Nature* **426,** 33–38
25. Lim, J. H., Kim, M. S., Kim, H. E., Yano, T., Oshima, Y., Aggarwal, K., Goldman, W. E., Silverman, N., Kurata, S., and Oh, B. H. (2006) *J. Biol. Chem.* **281,** 8286–8295
26. Chang, C. I., Chelliah, Y., Borek, D., Mengin-Lecreulx, D., and Deisenhofer, J. (2006) *Science* **311,** 1761–1764
27. Zhang, R., Cho, H. Y., Kim, H. S., Ma, Y. G., Osaki, T., Kawabata, S., Söderhäll, K., and Lee, B. L. (2003) *J. Biol. Chem.* **278,** 42072–42079
28. Park, J. W., Je, B. R., Piao, S., Inamura, S., Fujimoto, Y., Fukase, K., Kusumoto, S., Söderhäll, K., Ha, N. C., and Lee, B. L. (2006) *J. Biol. Chem.* **281,** 7747–7755
29. Park, J. W., Kim, C. H., Kim, J. H., Je, B. R., Roh, K. B., Kim, S. J., Lee, H. H., Ryu, J. H., Lim, J. H., Oh, B. H., Lee, W. J., Ha, N. C., and Lee, B. L. (2007) *Proc. Natl. Acad. Sci. U.S.A.* **104,** 6602–6607
30. Kim, C. H., Kim, S. J., Kan, H., Kwon, H. M., Roh, K. B., Jiang, R., Yang, Y., Park, J. W., Lee, H. H., Ha, N. C., Kang, H. J., Nonaka, M., Söderhäll, K., and Lee, B. L. (2008) *J. Biol. Chem.* **283,** 7599–7607
31. Roh, K. B., Kim, C. H., Lee, H., Kwon, H. M., Park, J. W., Ryu, J. H., Kurokawa, K., Ha, N. C., Lee, W. J., Lemaitre, B., Söderhäll, K., and Lee, B. L. (2009) *J. Biol. Chem.* **284,** 19474–19481
32. Lee, K. Y., Zhang, R., Kim, M. S., Park, J. W., Park, H. Y., Kawabata, S., and Lee, B. L. (2002) *Eur. J. Biochem.* **269,** 4375–4383
33. Moon, H. J., Lee, S. Y., Kurata, S., Natori, S., and Lee, B. L. (1994) *J. Biochem.* **116,** 53–58
34. Kan, H., Kim, C. H., Kwon, H. M., Park, J. W., Roh, K. B., Lee, H., Park, B. J., Zhang, R., Zhang, J., Söderhäll, K., Ha, N. C., and Lee, B. L. (2008) *J. Biol. Chem.* **283,** 25316–25323
35. Bulet, P., Hetru, C., Dimarcq, J. L., and Hoffmann, D. (1999) *Dev. Comp. Immunol.* **23,** 329–344
36. Tsuchiya, M., Asahi, N., Suzuoki, F., Ashida, M., and Matsuura, S. (1996) *FEMS Immunol. Med. Microbiol.* **15,** 129–134
37. Yoshida, H., Ochiai, M., and Ashida, M. (1986) *Biochem. Biophys. Res. Commun.* **141,** 1177–1184
38. Mellroth, P., Karlsson, J., Håkansson, J., Schultz, N., Goldman, W. E., and Steiner, H. (2005) *Proc. Natl. Acad. Sci. U.S.A.* **102,** 6455–6460
39. Jiang, R., Kim, E. H., Gong, J. H., Kwon, H. M., Kim, C. H., Ryu, K. H., Park, J. W., Kurokawa, K., Zhang, J., Gubb, D., and Lee, B. L. (2009) *J. Biol. Chem.* **284,** 35652–35658
40. Liu, L., Roberts, A. A., and Ganz, T. (2003) *J. Immunol.* **170,** 575–580
41. Becker, M. N., Diamond, G., Verghese, M. W., and Randell, S. H. (2000) *J. Biol. Chem.* **275,** 29731–29736

SUPPLEMENTAL MATERIALS

Diversity of innate immune recognition mechanism for bacterial polymeric *meso*-diaminopimelic acid-type peptidoglycan in insects

Yang Yu, Ji-Won Park, Hyun-Mi Kwon, Hyun-Ok Hwang, In-Hwan Jang, Akiko Masuda, Kenji Kurokawa, Hiroshi Nakayama, Won-Jae Lee, Naoshi Dohmae, Jinghai Zhang, and Bok Luel Lee*

* To whom correspondence should be addressed. E-mail: brlee@pusan.ac.kr

This file includes supplemental Table 1 and Figures S1 –S4.

Table 1. Quantitative amino acid composition of the DAP-type PGs from *E. coli* and *B. subtilis*

Amino acid	Amino acid quantities / 1 μg DAP-type PG (pmol)	Normalized to (Alanine=2.0)
	E. coli / B. subtilis	*E. coli / B. subtilis*
Diaminopimelic acid	90.4 / 90.2	1.1 / 1.1
Muramic acid	43.1 / 43.2	0.5 / 0.5
Glucosamine	25.3 / 25.1	0.3 / 0.3
Phenylalanine	2.5 / 2.1	0.0 / 0.0
Cystenine	0.2 / 0.1	0.0 / 0.0
Leucine	5.1 / 5.0	0.1 / 0.1
Isoleucine	2.8 / 2.9	0.0 / 0.0
Lysine	9.0 / 9.2	0.1 / 0.1
Methionine	0 / 0	0.0 / 0.0
Valine	3.6 / 3.8	0.0 / 0.0
Tyrosine	1.6 / 1.1	0.0 / 0.0
Glutamic acid	96.6 / 96.2	1.2 / 1.2
Aspartic acid	7.6 / 7.1	0.1 / 0.1
Alanine	160.9 / 161.1	2.0 / 2.0
Proline	1.8 / 2.1	0.0 / 0.0
Threonine	2.4 / 2.5	0.0 / 0.0
Glycine	8.2 / 8.1	0.1 / 0.1
Serine	6.5 / 6.3	0.1 / 0.1
Histidine	0.8 / 0.6	0.0 / 0.0
Arginine	7.4 / 7.1	0.1 / 0.1

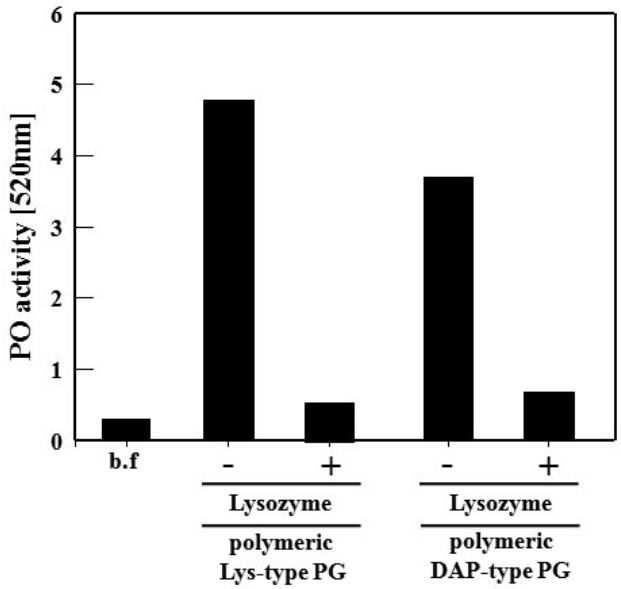

Figure S1. Measurements of PO activities by lysozyme treated-polymeric Lys-type and DAP-type-PGs in *Tenebrio* hemolymph. To measure PO activity, 30 μl of crude hemolymph (150 μg of proteins) was preincubated in 85 μl of 20 mM Tris-HCl buffer (pH 8.0) containing 1 μg of polymeric PGs or lysozyme-treated PGs for 10 min at 30°C, and then 400 μl of substrate solution (1 mM 4-methylcatechol, 2 mM 4-hydroxyproline ethylester in 20 mM Tris-HCl buffer, pH 8.0, containing 5 mM $CaCl_2$) was added to the reaction mixture. After incubation at 30°C for 10 min, the increase in absorbance at 520 nm was measured using a Shimadzu spectrophotometer. One unit of PO activity was defined as the amount of enzyme causing an increase in absorbance of 0.1 at 520 nm per 10-min incubation (A_{520}/10 min).

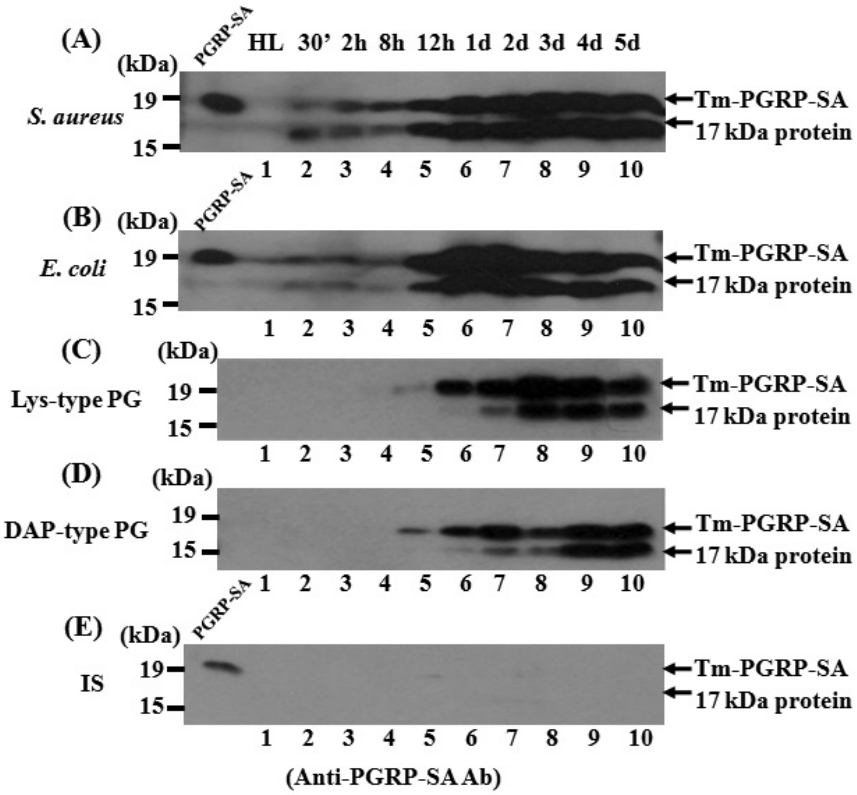

Figure S2. The amounts of *Tenebrio* PGRP-SA and 17-kDa protein in the hemolymph increased after injection of bacteria and PGs.

(A), (B), (C), (D) and (E) represent the Western blot analyses by using anti-PGRP-SA antibody after injection of *S. aureus* ($2x10^6$ cells/larva), *E. coli* ($2x10^6$ cells/larva), polymeric *S. aureus* Lys-type PG (100 ng/larva), polymeric *E. coli* DAP-type PG (100 ng/larva) and insect saline (IS) (4 μl), respectively. On indicated times, hemolymph was collected and then a portion (50 μg of protein) of each sample was analyzed by immunoblotting using affinity-purified anti-*Tenebrio* PGRP-SA antibody.

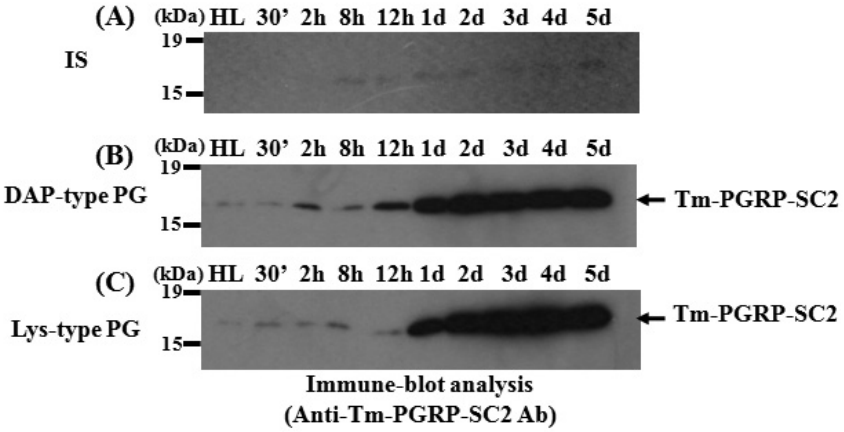

Figure S3. The amounts of *Tenebrio* PGRP-SC2 in the hemolymph increased after injection of polymeric PGs.

(A), (B) and (C) represent the Western blot analyses by using anti-PGRP-SC2 antibody after injection of insect saline (IS, 4 μl), polymeric *S. aureus* Lys-type PG (100 ng/larva), and polymeric *E. coli* DAP-type PG (100 ng/larva), respectively. On indicated times, hemolymph was collected and then a portion (50 μg protein) of each sample was analyzed by immunoblotting using affinity-purified anti-*Tenebrio* PGRP-SC2 antibody.

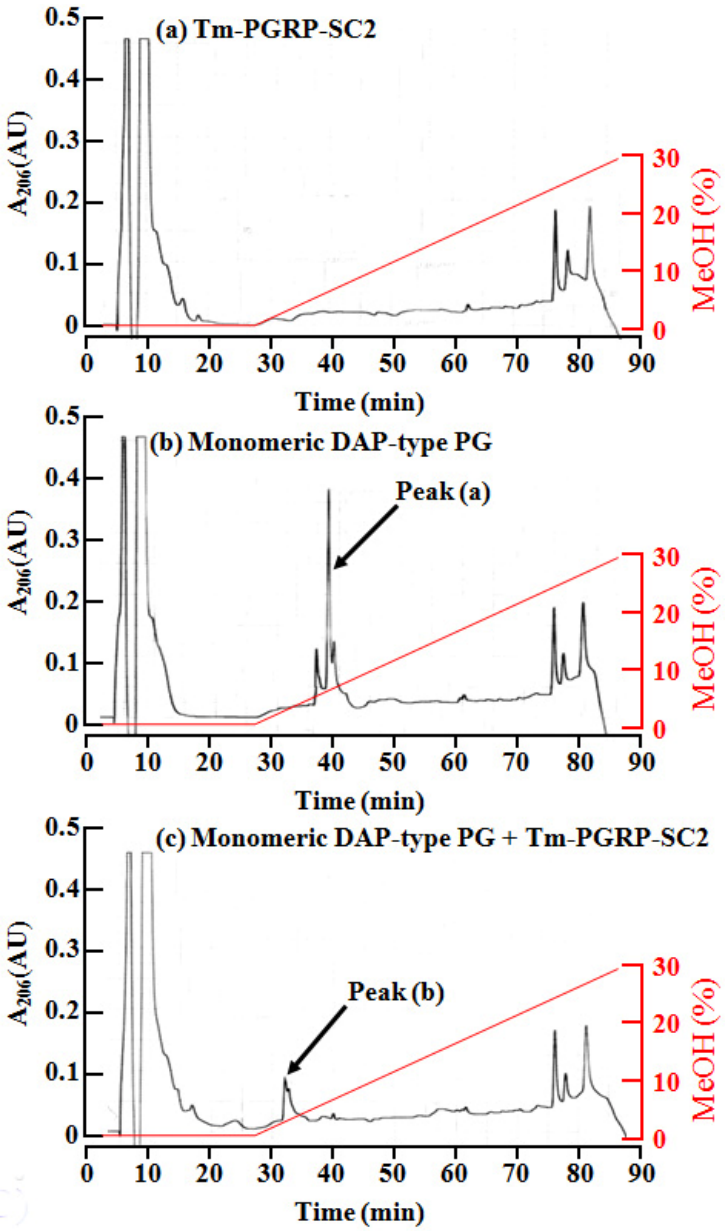

Figure S4. HPLC elution patterns of lysozyme-treated DAP-type PG and PGRP-SC2-treated monomeric DAP-type PG. (A), (B) and (C) represent the elution profile after injection of *Tenebrio* PGRP-SC2, the reaction mixture of lysozyme-treated DAP-type and the reaction mixture of PGRP-SC2 and peak (a), respectively. Polymeric DAP-type PG (600 μg) and lysozyme (100 μg) were incubated for 16 h at 37°C and then the supernatant was fractionated using a Hydrosphere C18 (4.6 x 250 mm I.D.) column with methanol gradient (shown on the *right-hand side*). The major peak (peak a) was again incubated with recombinant PGRP-SC2 (10 μg) for 6 h at 30°C. The mixture was again injected to the same HPLC column and then peak (peak b) was collected and then analyzed by Edman reaction on the automatic amino acid sequencer.